

LETTER

Electrically-latched compliant jumping mechanism based on a dielectric elastomer actuator

To cite this article: M Duduta *et al* 2019 *Smart Mater. Struct.* **28** 09LT01

View the [article online](#) for updates and enhancements.

Letter

Electrically-latched compliant jumping mechanism based on a dielectric elastomer actuator

M Duduta^{1,2} , F C J Berlinger^{1,2}, R Nagpal^{1,2}, D R Clarke¹, R J Wood^{1,2} and F Zeynep Temel^{1,2,3} 

¹Harvard Paulson School of Engineering and Applied Sciences, 9 Oxford St., Cambridge, MA 02138, United States of America

²Wyss Institute for Biologically Inspired Engineering, 60 Oxford St., Cambridge, MA 02138, United States of America

³Robotics Institute at Carnegie Mellon University, 5000 Forbes Avenue, Pittsburgh, PA 15213, United States of America

E-mail: mduduta@g.harvard.edu

Received 15 March 2019, revised 13 June 2019

Accepted for publication 24 July 2019

Published 12 August 2019



CrossMark

Abstract

Jumping mechanisms are useful in robotics for locomotion in unstructured environments, or for self-righting abilities. However, most rigid robots rely on impact with the ground to jump, thereby requiring a relatively rigid, and flat environment. Moreover, they need to be able to absorb high impact forces during landing in order to maintain structural integrity. In this paper we investigate soft systems, capable of jumping repeatedly in unstructured environments with no need for precise landings. Our impulsive approach is based on a soft electro-mechanical transducer, a dielectric elastomer actuator (DEA). The design is inspired by click-beetles and simple bio-mechanical models, which convert the flexing around a hinge into jumping. Our actuator is power amplified by the addition of a stiffer strip, allowing for rapid shape transitions (22 ms) between flat and curved states. The transition is controlled by an electric latch: the DEA is discharged faster than the actuator can deform. The mechanical energy stored in the composite beam is released rapidly, leading to impulsive motions (jumps of a full body length: i.e. 5 cm). This demonstration of an electrically-latched power amplification mechanism shows that relatively simple electro-mechanical systems can exhibit impulsive behavior which may enable new types of locomotion in compliant machines.

Supplementary material for this article is available [online](#)

Keywords: soft robotics, dielectric elastomer actuator, power amplification, jumping mechanism, jumping robot

(Some figures may appear in colour only in the online journal)

1. Introduction

Robots which have the ability to jump make use of power amplification mechanisms to bypass the universal trade-off between force and velocity [1] to overcome obstacles larger

than their step size [2] and for self-righting abilities [3]. Most typically, the energy output of a muscle or actuator is used to deform a spring, which is held in place by a mechanical latch, therefore storing mechanical energy. When the mechanical latch is removed, the energy stored in the spring is released

faster than the muscle or actuator can deform, increasing the power output of the system. By comparison, the electrical latch described in this work is a capacitor that can transition between its charged and discharged states without any moving mechanical parts. In conjunction with an electro-mechanical transducer, this electrical latch enables impulsive motions in simple systems with a single moving part. To store energy in a power-amplifying mechanism, most jumping robots employ motors or actuators made of high stiffness materials, including DC motors [4], shape memory alloys (SMAs) [5], and electrostatic inchworm motors [6].

While there are multiple engineering solutions for jumping mechanisms made of rigid components, few options exist for jumping mechanisms in soft robots [7]. A bio-inspired approach uses pneumatic actuators as artificial muscles, while springs serve as the energy storing element [8]. To bypass the need for springs, a different approach uses combustion of ignitable gases to create large and rapid volume changes [9]. Some limitations of this approach (e.g. high stress concentrations) can be addressed by 3D printing a gradient in stiffness across the robot body, from the soft deformable ‘feet’ to the rigid chassis which encases the power electronics and fuel containers [10]. The same idea of using low viscoelasticity silicone elastomers as the energy storing spring, can be employed at smaller scales [11]. Several hybrid approaches use flexible SMA coils to achieve jumping in laminated structures [12], and soft, elastomeric bodies [13], as well as ballistic rolling in caterpillar-inspired robots [14]. From all of these examples, two ideas emerge as guidelines for designing a jumping mechanism based on soft materials: (1) soft elastomers can be used as energy-storing springs, and (2) having an electrically-powered actuator simplifies the robot design, bypassing the need for pumps or ignition mechanisms.

A suitable technology for such soft jumping mechanisms are dielectric elastomer actuators (DEAs), which are compliant capacitors that can convert electrical energy into mechanical work [15]. With the exception of a limited hop [16], DEAs have never been used to power jumping robots because of either their low energy density, or slow response speeds [17]. Recent advances in DEA fabrication and materials have enabled multilayer actuators which deform without pre-stretch [18] and exhibit specific energy on par with natural muscles [19]. These actuators have been used in robotic demonstrations, including crawling inchworms [20], and autonomous swimming robots [21]. However, despite significant improvements in the response speed of DEAs [22], in direct-drive configuration DEAs alone cannot achieve speeds or energy release rates that are conducive to jumping. For example, the silicone roll actuators described in [22] when driven by a step input are only capable of hops in the range of 1%–10% of body lengths, less than the linear displacement of a roll. Therefore a challenge remains to integrate a power amplification mechanism with a DEA to enable jumping motion.

The majority of jumping mechanisms in natural and engineered systems rely on pushing against the ground to achieve impulsive motion [1]. One type of insect, the click

beetle, is unique in jumping because it is capable of jumping without using its legs [23], regardless of the orientation of its body. The click beetle has a hinged body and can rapidly transition from a flat to a bent state. When the beetle body is pointing down and its legs touch the ground, closing the hinge rapidly pushes against the ground to induce jumping. However, the beetle rarely exhibits this type of motion [24]. Instead, the beetle uses the rapid jack-knifing of the body when pointing upwards and its legs are not in contact with the ground, as a means of self-righting [25]. Simple beams with hinges have been shown to be useful bio-mechanical models [26] that replicate this jumping mechanism. Taking inspiration from the click beetle, we aim to demonstrate a mechanism capable of jumping from both orientations of the body, to enable richer locomotion modes and potentially robots capable of self-righting.

In this paper we show how a jumping mechanism is made by using the conventional frame of a DEA as a power amplification mechanism. Most DEAs are made by pre-stretching an elastomer and attaching it to a rigid frame. The motivation for using a support frame in DEAs is to increase both the range of electric-field induced deformation, as well as the breakdown strength [27]. Some approaches use flexible frames to set a specific minimum energy state, as well as a deformation path for the DEA between the actuated and the relaxed states [28]. One advantage to this approach is the ability to shuttle mechanical energy from the elastomer to the frame and back depending on the level of strain in the elastomer. Here we replace an external frame with a thin, much stiffer elastic strip to form a residually stressed bi-layer composite beam. As will be described in the following, recoverable mechanical energy can be stored by bending and unbending the stiffer layer, depending on voltage applied to the actuator. The system has a built-in electric latch, which is unique for engineered systems because it reduces the number of moving mechanical parts: when the DEA capacitor is rapidly discharged, the beam returns to its original bent state, generating an impulsive motion which can power a jumping mechanism. A schematic of how energy is shuttled between mechanical, electrical, and kinetic energy is shown in figure 1. We focus on the deformation of a bi-layer composite beam because it is both simple to analyze and has a geometry that allows the energy released to be converted into vertical motion.

The first part of the paper covers two simple models of the system: the first model focuses on the material and geometric parameters that govern its shape when at equilibrium as a function of applied initial strain to the elastomer. The second model focuses on how the shape of the actuator changes as a function of the applied voltage. The next part briefly describes how the actuator is fabricated, using insight from the first model. Lastly, jumping from both orientations is demonstrated and future directions are discussed.

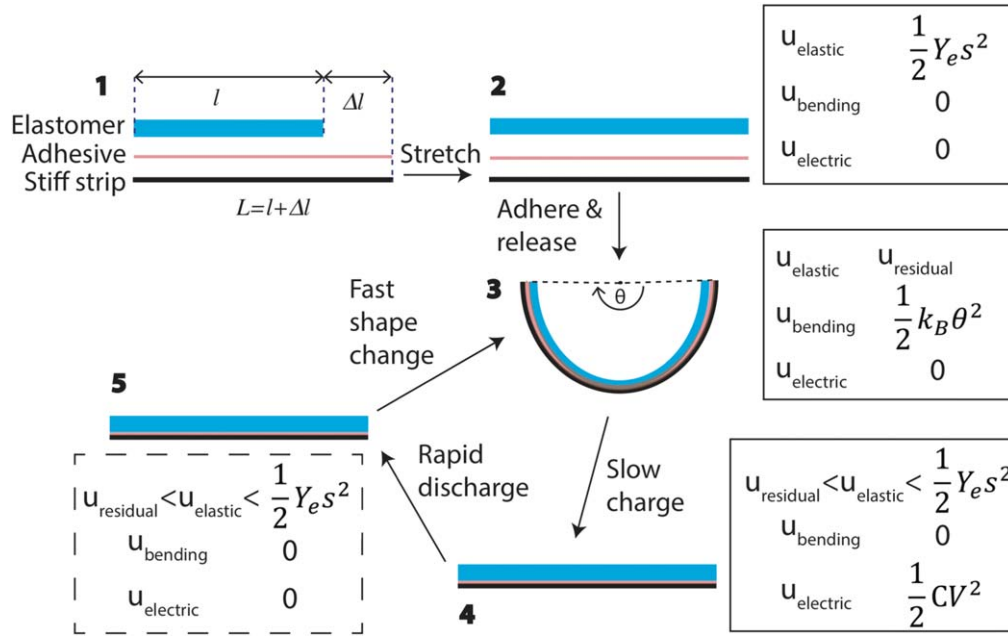


Figure 1. Jumping beam energy conversion steps. (1) The starting materials are mismatched in terms of length: the elastomer length is l , while the thin stiff strip is of length $L = l + \Delta l$. (2) The elastomer (with Young's modulus of Y_e) is pre-stretched to reach the same length as the stiff strip. (3) The elastomer is adhered to the stiff strip creating residual stresses in both strips. When the composite bi-layer beam is released, it bends to minimize its elastic energy. The bending angle of the composite beam is Θ , and the bending spring constant is k_B . (4) Charging the DEA produces a Maxwell stress, stretching the elastomer that acts to decrease the bending of the beam. The actuator of capacitance C is charged to a voltage V . (5) Discharging the capacitance of the charged elastomer by shorting the electrodes allows the bi-layer beam to spring back to its fully bent configuration. The dashed line is meant to indicate this is an unstable, transition state. The rapid shape change accelerates the center of mass upwards, causing the beam to jump. The energy conversion cycle can be repeated by re-charging the elastomer to store mechanical energy and prime the jumping mechanism.

2. Modeling and design

In this section, two simple models are developed: the first is used to guide the design and material selection of the jumping mechanism, the second is used to provide some understanding of shape changes as a function of applied voltage on the DEA.

The first model is developed along similar lines as existing work on bi-material cantilevers [29, 30]. Here we use linear elasticity, as the strains in the materials are relatively small ($<30\%$) and therefore we expect infinitesimal strain theory to apply. The goal is to find a set of material and geometric parameters that will take a curved shape at equilibrium, aiming for a full circle (360°). Larger angles will cause the composite to bend on itself, potentially causing self-adhesion and preventing movement. A full derivation of this first model is presented and verified in the supplemental information section is available online at stacks.iop.org/SMS/28/09LT01/mmedia. The model is used to predict the bend angle as a function of length, width, and thickness of each material, as well as their Young's moduli and initial strain applied to the elastomer.

Conceptually, we input mechanical energy by pre-stretching a soft elastomer strip of initial length, l , and attach it to a thin, elastic strip of length, L . The strain, s , is generated in the same direction as the applied stress (i.e. along the length). The mechanical energy required to stretch the elastomer strip

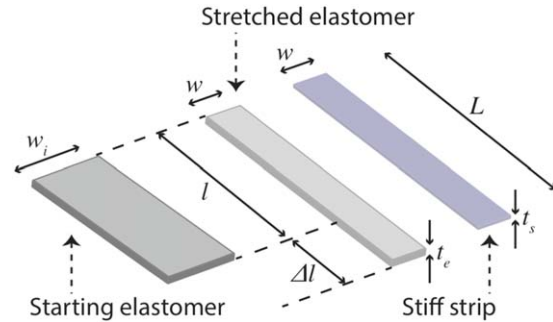


Figure 2. Geometric parameters for the elastomer and stiff strip. The elastomer strip starts in a relaxed state (left), then is stretched uniaxially (middle) by a strain of $s = \Delta l$ to match the length (L) and width (w) of the stiff strip (right).

by a strain, s , is given by:

$$U_{\text{stretch}} = \frac{s^2 Y_e L w t_e}{2} \quad (1)$$

where s is the applied strain to the elastomer, Y_e is the Young's modulus of the elastomer, l is the length of the elastomer before strain is applied, w is the width of the elastomer, t_e is its thickness (figure 2) in the stretched state. After bonding the stretched elastomer strip to the thin layer and the bi-layer is released of any constraints, it will both bend and compress to reduce its total elastic strain energy.

From here, we consider only the bending energy of the stiff strip to build the second model and predict deformation

of the composite when voltage is applied. The stiff substrate has a high Young's modulus relative to that of the elastomer, making it practically inextensible, but capable of bending to store mechanical energy. The bending energy in the stiff strip can be approximated using the same principles from [28]:

$$U_{bending} = \frac{Y_s w t_s^3}{24L} \Theta^2, \quad (2)$$

where Y_s is the Young's modulus of the stiff strip, w , t_s , and L are the width, thickness, and the length of the stiff strip, respectively, while Θ is the bending angle at equilibrium.

When an electric field is applied across the elastomer, electrical energy is provided by a power supply to the elastomer strip. This electrical energy is given by:

$$U_{electrical} = \frac{CV^2}{2}, \quad (3)$$

where C is the capacitance of the DEA, and V is the applied voltage on the entire stack. To a first approximation, in the limits of small strains, we consider the width and length of the capacitor to not change significantly during charging. Since the first model helped select both the total thickness of the elastomer, t_e , and the number of layers in the dielectric elastomer, N , the thickness of each individual layer in the DEA is equal to $t_{layer} = t_e/N$. For each layer making up the DEA, the capacitance is equal to

$$C_{layer} = \frac{\epsilon \epsilon_0 w L}{t_{layer}} = \frac{N \epsilon \epsilon_0 w L}{t_e}, \quad (4)$$

where ϵ is the dielectric constant of the elastomer (approximated to be $\epsilon = 4$ based on earlier work [31]), ϵ_0 is the permittivity of free space ($\epsilon = 8.85 \times 10^{-12} \text{ m}^{-3} \text{ kg}^{-1} \text{ s}^4 \text{ A}^2$), w is the width of the capacitor, L is the length of the elastomer, N is the number of layers, and t_e is the thickness of the elastomer. Since there are N layers in the dielectric elastomer, the total capacitance of the multilayer DEA is $C = N C_{layer}$. As a result, the total electrical energy input has the following formula:

$$U_{electrical} = \frac{CV^2}{2} = \frac{N C_{layer} V^2}{2} = \frac{N^2 \epsilon \epsilon_0 w L V^2}{2 t_e}. \quad (5)$$

The electromechanical coupling between charges on opposite electrodes causes a Maxwell stress that acts to compress the elastomer in its thickness direction and elongate the elastomer strip. This Maxwell stress causes the elastomer to stretch, making its length closer to that of the stiff strip, and thus reducing the amount of bending in the bi-layer beam. However, dielectric elastomers are not perfect electromechanical transducers, and only a small part of the input electrical energy is converted into mechanical work that counteracts the initial bending in the beam. That electromechanical efficiency, η , can be estimated from previous work [19], and by comparing the model predictions to observed experimental results. Using the initial bending energy (which depends on the resting angle Θ), the input electrical energy (which depends on the applied voltage V), we obtain the following relationship that links shape of the

charged DEA ($\Theta_{charged}$) to the applied voltage:

$$U_{bending} - \eta U_{electrical} = \frac{Y_s w t_s^3}{24L} \Theta_{charged}^2. \quad (6)$$

If the capacitor is discharged, the elastomer contracts, restoring the bi-layer beam to the initial fully-bent state. As it does so, the beam geometry dictates that the center of mass moves upwards. When this discharge occurs rapidly, the acceleration of the center of mass can propel the beam into the air, converting some of the stored mechanical energy into kinetic energy for jumping.

We used the first part of the model as a guide for building a mesoscale jumping mechanism. To size the device, we focused only on the upper end of typical lengths of click beetles ($L = 5 \text{ cm}$ from [23]). From existing work [1] we know that smaller devices can deliver higher specific power, but were limited in how much we could reduce the size of the DEA because of fabrication constraints, in particular making reliable electrical connections in electrodes with small features. For practical considerations, we limited the choice of elastomer and stiff strip, and only modified the geometry of each component. Our inputs were the thicknesses of the elastomer and the stiff strip, the number of layers in the elastomer, the length and width of the final bi-material beam, and the amount of electrical energy input in the actuator. We made the stiff strip and elastomer with the same aspect ratio and dimensions (length of $5 \text{ cm} \times$ width of 2 cm). These dimensions are that of the stiff strip, and the elastomer was sized accordingly to fit the dimensions in its stretched state.

The design is partly inspired by a rigid bio-mechanical model of the click beetle [26]. Their model indicates that by flexing a cantilever beam rapidly, most of the mechanical energy is released as a force pushing against the ground at the hinge point, which is sufficient for jumping. To mimic this behavior in a compliant mechanism, our design target was a bi-material beam which would have a resting full circle shape, corresponding to $\theta = 360^\circ$. When powered, the target cantilever would reach a flat shape at an applied field of $125 \text{ V } \mu\text{m}^{-1}$, near the upper limit of what these DEAs can withstand.

The material and geometric parameters selected are listed in table S1. The elastomer Young's modulus can be matched by an established acrylic chemistry with 7.5% HDDA crosslinker [18], while the Young's modulus of the stiff strip can be matched by readily available Mylar sheets. The predicted behavior when transitioning between actuated and relaxed states is shown in figure 3. The input electrical energy depends on the square of the applied voltage, meaning more deformation is predicted at high fields, which is confirmed by visual observations (figure S3). As the elastomer has a 1 mm thickness and is made of 24 layers, each individual layer has a thickness of $41 \text{ } \mu\text{m}$, corresponding to $125 \text{ V } \mu\text{m}^{-1}$ at an applied voltage of 5 kV, close to the breakdown limit of these multilayered systems [19].

In addition to storing mechanical energy by bending, the stiff strip also increases the speed with which the energy is released. Given the simple construction and geometry, the elastomer and stiff strip composite structure can be considered

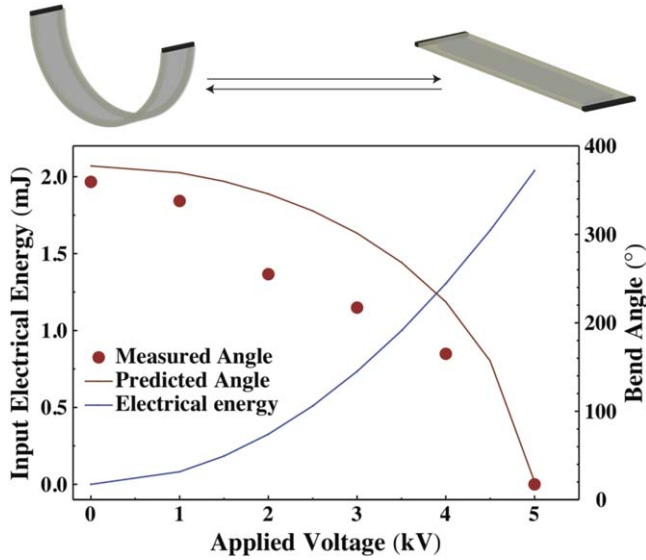


Figure 3. Energy states in a pre-stretched composite beam. Dependence of the electrical energy input into the system as a function of applied voltage (left y-axis). The elastomer had been pre-stretched 20% of its initial length before attaching the stiff strip. The applied voltage allows the structure to switch between two states: a circular beam at 0 kV and a flat beam at 5 kV. Dependence of the shape of the bi-layer beam on the applied voltage. The predicted angle corresponds to the bend angle of the bi-layer beam, Θ when no voltage is applied, and $\Theta_{charged}$ at the instances where voltage is applied on the DEA, calculated using equation (6) for an electromechanical efficiency of $\eta = 0.8\%$. The measured angle is extracted from images of the beam during charging (figure S3).

to be a bi-material beam. To a first degree, the response speed can be taken to be proportional to the first frequency of vibration of the cantilever [32]. From [33] we know that the ratio of the frequency of vibration of the bi-material beam and the frequency of the elastomer-only beam can be estimated as

$$\left(\frac{f_{bim}}{f_e}\right)^2 = \left[\frac{(1 + E_r h_r)(1 + E_r h_r^3) + 3E_r h_r(1 + h_r)^2}{(1 + \rho_r h_r)(1 + E_r h_r)}\right], \quad (7)$$

where $E_r = Y_s/Y_e$, is the ratio of the Young's moduli of the stiff strip and the elastomer, $h_r = t_s/t_e$ is the ratio of the thicknesses of the stiff strip and the elastomer, and ρ_r is the ratio of the densities of the stiff strip and the elastomer. For the jumping demonstration in figure 6, the ratios are as follows:

$E_r = 2 \times 10^9 / 3 \times 10^5 = 6,666$,
 $h_r = 0.0003 / 0.001 = 0.3$ and $\rho_r = 1$. The resulting boost in frequency is $f_{bim}/f_e = 12$, meaning the energy can be released 12 times faster because of the addition of a stiff strip. We note that the resonant frequency of the beam is only an approximation, as under-damped beams can respond more quickly.

3. Fabrication

The multilayering process [18] was adapted to make multilayer DEA strips of a prescribed form factor. The composition of the acrylic elastomer was 70% oligomer CN9018 (from Arkema, Dallas, TX), mixed with 15% isodecyl acrylate,

7.5% hexanediol diacrylate, 5% isobornyl acrylate, 1% trimethylol propane triacrylate, 1% 2,2-bis(hydroxymethyl) propionic acid, and 0.5% benzophenone (all from Sigma Aldrich, St. Louis, MO). The electrodes were made by stamping mats of carbon nanotubes (CNTs) supported by polytetrafluoroethylene (PTFE) filters directly onto the elastomers. The mats were prepared by filtering aqueous CNT inks (from Nano-C, Westwood, MA) diluted with isopropanol through PTFE membranes (Spectrum, 0.2 μm pore size). The multilayer actuators are made by a sequence of consecutive spin coating (Laurell Technologies) and curing of the elastomers, alternating with stamping of the CNTs through masks to form interdigitated power and ground electrodes. The acrylic elastomer layers were cured by exposure to UV light (365 nm wavelength) for 2 min for each layer.

For the elastomer we chose the composition of CN9018 with 7.5% HDDA crosslinker. This elastomer composition has Young's modulus comparable to natural muscle (300 kPa) [34], and an ability to sustain strains of 50% its initial length without breaking, which allows for large amounts of mechanical energy to be stored by pre-stretching. For reference, the Young's modulus of this elastomer is approximately half that of resilin (588 kPa in the hydrated state), one of the elastic proteins that enable jumping in a wide range of insects [35]. The areal electrode densities were all set to 15.59 $\mu\text{l cm}^{-2}$ to minimize the likelihood of dielectric breakdown at high applied electric fields. The areal density of ink corresponds to 300 μl ink at 17% optical transmittance [36] filtered through a PTFE membrane of 7 cm diameter. The completed and cured elastomer strips were then stretched using an Instron mechanical tester to the target strain ($s = 30\%$) and held in place by fixtures. An adhesive (CN9018 with 0% HDDA crosslinker) was used to bond the elastomer to the stiff material (polyethylene terephthalate glycol (PETG) for the demonstration in figure 6 and Mylar for the demonstration in figure 7) as described in figure 4. After the stiff layer was adhered, the elastomer was released from the fixtures, and the inactive ends were cut to make electrical connections to the power and ground electrodes of the actuator. As shown in earlier work [19], the conversion efficiency for multilayer DEAs is relatively small; to match values expected from earlier work, we considered $\eta = 0.8\%$ and obtained good agreement between the model and experimental results.

4. Demonstration

Using the model guidance we fabricated elastomer-stiff strip composite beams, with the goal of demonstrating successful jumps. To our knowledge, until now there have been no successful demonstrations of DEA robots which can jump to a height greater than one body length. The deformation of the DEA jumpers was recorded using a high speed camera (Phantom v7.3 from Vision Research, Wayne, NJ). The images were captured at 6688 frames per second, and a resolution of 800 \times 600 pixels. The DEA was powered to 5–8 kV using a high voltage amplifier (Trek, Lockport, NY).

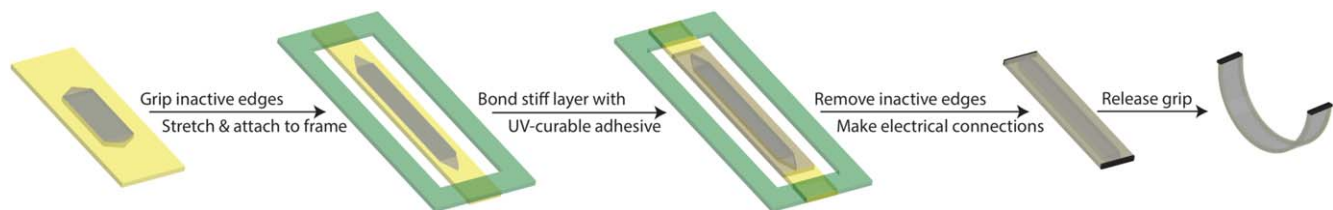


Figure 4. Fabrication of pre-stretched structure. The multilayer elastomer actuator starts in a relaxed state. We grip the inactive edges and apply the desired strain level to the elastomer. With the elastomer still in the strained state we apply uncured adhesive and a stiff strip to one side of the elastomer. After curing the adhesive, the grips are removed and the inactive sections are cut which leads to a curved elastomer-stiff strip minimum energy structure.

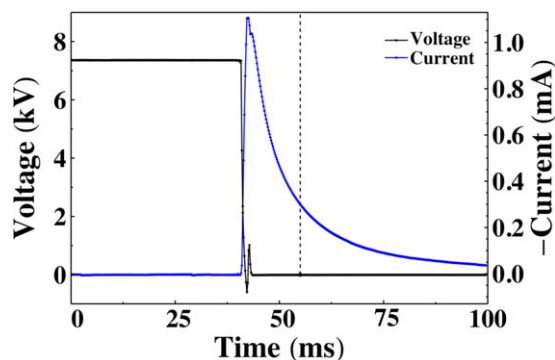


Figure 5. Voltage and current response. Plot of the voltage applied to the actuator (left y-axis), and the response current (right y-axis) as a function of time. The dashed line corresponds to one t_{RC} interval (15 ms) from when the voltage is switched off. The data shows that the voltage slew rate of the power supply is high, and the target voltage is reached within 4–6 ms. The current drops to less than 40% of the maximum (1.1 mA) within 15 ms, as expected based on measurements of resistance and capacitance.

From its fully charged state the actuator was discharged by switching the power supply from the maximum applied voltage to 0 kV, with a current limit of ± 2 mA. An example step discharge and the corresponding current are shown in figure 5. The results indicate that the high voltage power supply has a high voltage slew rate and is not a rate limiting element.

Two demonstrations are presented in this section from two different actuators. Actuator 1, captured in figure 6 and in supplemental video S1, uses PETG as the stiff material ($Y_s = 2$ GPa at a thickness of $t_s = 300$ μm), and is charged to a maximum of 8 kV. Actuator 2, captured in figure 7, and in supplemental video S2 uses mylar as the stiff material ($Y_s = 7$ GPa at a thickness of $t_s = 75$ μm), and is charged to a maximum of 5 kV. The widths of the actuators are different (actuator 1 has a width of 1 cm, while actuator 2 has a width of 2 cm), while other parameters of the device are the same across the two actuators, and are summarized in supplemental table S1. The captured images in figure 6 show that actuator 1 is able to complete a jump of approximately one body length in less than 0.2 s.

The potential energy in the jumping composite beam in figure 6 can be estimated from its mass and the maximum height reached. In this example the beam reaches a height of $h = 5$ cm for a mass of 2 g. The potential energy at the peak of the jump is

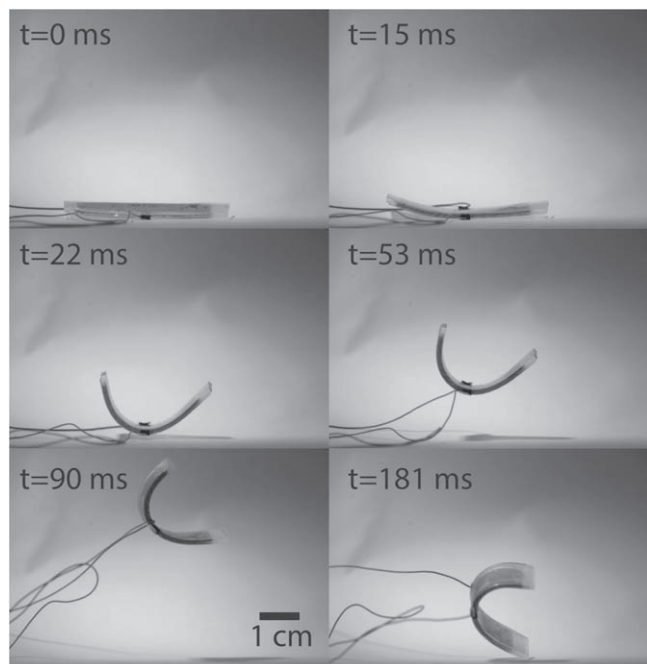


Figure 6. Jump demonstration. Six instances throughout the jump of a DEA powered mechanism. The entire jump between when the capacitor is discharged and the mechanism makes contact again with the ground takes less than 0.2 s. The jump bears some resemblance to jumping observed in click beetles, in which a flat body crunches and pushes against the ground to cause jumping.

$u_{pot} = mgh = 2g \cdot 9.8 \text{ m s}^{-2} \cdot 5 \text{ cm} = 0.98 \text{ mJ}$. Therefore the power released during the jump corresponds to the ratio of energy to the release time, in this case taken to be 22 ms, from when the capacitor is discharged to when it reaches its relaxed state configuration. Accordingly, the power in the system is estimated to be 44.5 mW, and the specific power of the mechanism is 22.5 W kg^{-1} . In terms of efficiency, most of the energy stored in bending the stiff strip (1.11 mJ, as estimated using the material parameters in equation (2)) is transferred as kinetic energy used for jumping (88% efficiency). Since the jump was partly limited by the electrical connection tethers, the transfer energy efficiency may be even higher, and closer to 100%. Given the high conversion efficiency, the model will be useful to predict jump heights or optimize the mechanism, for example by using a different stiff material to increase the jump height. However, the electro-mechanical energy conversion efficiency is low, as the actuator requires 8 kV to deform, meaning more than 400 mJ of electrical energy are

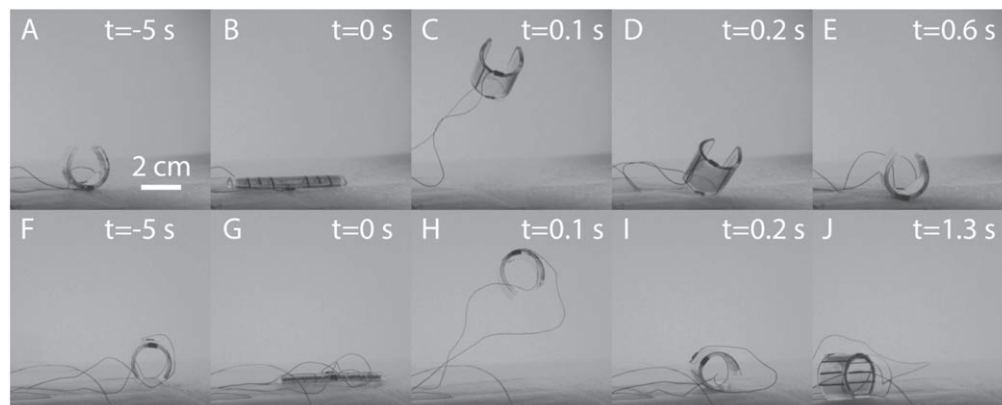


Figure 7. Jumps from different orientations. Five instances throughout the jump of a DEA powered mechanism in two separate orientations. The curved configuration at rest allows the device to roll after landing.

needed for 1 mJ of mechanical work. The low electro-mechanical efficiency is primarily due to resistive losses in the CNT electrodes (sheet resistances $>70 \text{ k}\Omega/\text{sq}$). As more conductive electrodes are developed for multilayer DEA devices, they could be used to increase the electro-mechanical efficiency of this jumping mechanism.

One of the key advances in this work is the use of an electric latch to control the release of mechanical energy from the system. Specifically, if the actuator is discharged faster than the elastomer can deform, there will be excess mechanical energy stored in the system and the speed of energy release will be determined only by the viscoelastic properties of the composite. In other words, the response speed is a function of both the viscoelastic properties of the elastomer as well as the capacitor discharge rate. Of the two, the slower process dominates and dictates what the response speed should be. To demonstrate impulsive motion in this section, we focused only on examples of discharging the actuator as fast as possible, to maximize the power output. A comparison between slower discharge rates is given in Supplemental figure S4, and shows that appreciable jumps are observed only at the fastest discharge rates. Given the material geometry and properties, the natural frequency of a beam made from the pure elastomer is approximately 4 Hz. By adding the stiffening element, according to equation (7), the natural frequency of the composite mechanism increases to 48 Hz, which corresponds to a period of 20.8 ms. This period set the upper limit for the target RC time constant, t_{RC} , of the capacitor. The dielectric constant of the elastomer used in the 24 layer actuator was measured to be 4, resulting in a theoretical capacitance value of 7.9 nF. The measured value for resistance was 1.2–1.6 M Ω , leading to estimated t_{RC} of 10–15 ms. The mechanism shown in figure 6 responds in 22 ms, very close to the predicted response speed of the composite. One potential limitation of this approach is the current required for fast discharge of the actuator. In our demonstration, the measured current was well below the maximum limit of the power supply (2 mA). For future untethered applications the power supply will need to be scaled appropriately to match the maximum power sink expected during discharge to produce impulsive motions.

As presented in the Introduction, the actuators have a curved resting state to allow for impulsive motions from either orientation of the beam: curved upwards or curved downwards relative to the flat ground. Actuator 2 demonstrates that the composite beam jumps from either orientation, as shown in figure 7. Frames A through E show a complete jump and return to equilibrium of a beam which points upward at rest. When energy is released by the electric latch, the ends of the beam move upwards rapidly, while the center of the beam pushes against the ground to cause takeoff. Alternatively, frames F through J show a complete jump and return to equilibrium of a beam which points downward at rest. When energy is released by the electric latch, the ends of the beam push against the ground to cause takeoff. Such a versatile device may be useful for studying different takeoff mechanisms in both natural and engineered systems. Additionally, the curved shape of the beam at rest allows the device to roll, as shown in the transition from I to J, which may enable other modes of locomotion. Repeated jumps from both orientations are shown consecutively in supplemental video S2. While the system is operated in open loop, there is potential for careful orientation of the body depending on how fast energy is stored and released from the system.

5. Conclusion



Here we report the first ever jumping mechanism driven by a power-amplified DEA. Among the unique features of this mechanism is the electric latch, which controls the release rate of stored elastic energy in the composite. The system is based on the combination of a soft electro-mechanical transducer with a stiff strip, and the mechanism can be easily integrated with other power electronics to build more complex and more capable soft robots, without requiring pumps or complex combustion chambers. The main advantages of this approach are the primarily soft body, that operates as an electro-mechanical transducer and therefore can release energy to cause impulsive motions without the need for moving parts in a mechanical latch. The main disadvantages are the low electro-mechanical efficiency, high resistance electrodes, as

well as high voltage required for deformation, all of which limit the ability to integrate this mechanism into a fully autonomous jumping robot. Still, these limitations are being addressed by multiple methods across different branches of materials and robotics. With integration of better materials as well as power electronics, expect this mechanism to be useful for multimodal locomotion [37], for example crawling and jumping over obstacles, or bio-inspired self righting motions [38]. While this first example is symmetric, simple modifications, such as usage of gradient stiffness materials, or different levels of pre-stretch in the elastomer, could be used to break symmetry, and give directionality to the jumps, further increasing the capability of the mechanism.

Acknowledgments

The research was supported by the National Science Foundation (Materials Research Science and Engineering Center, award no. DMR14-20570), the Army Research Office (award no. W911NF-15-1-0358) and the Wyss Institute for Biologically Inspired Engineering. Any opinions, findings, and conclusions or recommendations expressed in this material are those of the authors and do not necessarily reflect the views of the National Science Foundation.

ORCID iDs

M Duduta  <https://orcid.org/0000-0001-9965-9654>
F Zeynep Temel  <https://orcid.org/0000-0002-1241-3959>

References

- [1] Ilton M *et al* 2018 *Science* **360** eaao1082
- [2] Armour R, Paskins K, Bowyer A, Vincent J and Megill W 2007 *Bioinspir. Biomim.* **2** S65
- [3] Zhang J, Song G, Li Z, Qiao G, Sun H and Song A 2012 Self-righting, steering and takeoff angle adjusting for a jumping robot 2012 *IEEE/RSJ Int. Conf. on Intelligent Robots and Systems (IROS)* pp 2089–94
- [4] Kovac M, Fuchs M, Guignard A, Zufferey J C and Floreano D 2008 A miniature 7g jumping robot 2008 *IEEE Int. Conf. on Robotics and Automation, ICRA 2008* pp 373–8
- [5] Noh M, Kim S W, An S, Koh J S and Cho K J 2012 *IEEE Trans. Rob.* **28** 1007–18
- [6] Bergbreiter S and Pister K S 2007 Design of an autonomous jumping microrobot 2007 *IEEE Int. Conf. on Robotics and Automation* pp 447–53
- [7] Rus D and Tolley M T 2015 *Nature* **521** 467
- [8] Niiyama R, Nagakubo A and Kuniyoshi Y 2007 Mowgli: a bipedal jumping and landing robot with an artificial musculoskeletal system 2007 *IEEE Int. Conf. on Robotics and Automation* pp 2546–51
- [9] Shepherd R F, Stokes A A, Freake J, Barber J, Snyder P W, Mazzeo A D, Cademartiri L, Morin S A and Whitesides G M 2013 *Angew. Chem. Int. Ed.* **52** 2892–6
- [10] Bartlett N W, Tolley M T, Overvelde J T, Weaver J C, Mosadegh B, Bertoldi K, Whitesides G M and Wood R J 2015 *Science* **349** 161–5
- [11] Gerratt A P and Bergbreiter S 2012 *Smart Mater. Struct.* **22** 014010
- [12] Koh J S, Yang E, Jung G P, Jung S P, Son J H, Lee S I, Jablonski P G, Wood R J, Kim H Y and Cho K J 2015 *Science* **349** 517–21
- [13] Sugiyama Y and Hirai S 2006 *Int. J. Robot. Res.* **25** 603–20
- [14] Lin H T, Leisk G G and Trimmer B 2011 *Bioinspir. Biomim.* **6** 026007
- [15] Pelrine R, Kornbluh R, Pei Q and Joseph J 2000 *Science* **287** 836–9
- [16] Pei Q, Pelrine R, Rosenthal M A, Stanford S, Prahlah H and Kornbluh R D 2004 Recent progress on electroelastomer artificial muscles and their application for biomimetic robots *Smart Structures and Materials 2004: Electroactive Polymer Actuators and Devices (EAPAD)* vol 5385 (International Society for Optics and Photonics) pp 41–51
- [17] Plante J and Dubowsky S 2007 *Smart Mater. Struct.* **16** S227
- [18] Duduta M, Wood R J and Clarke D R 2016 *Adv. Mater.* **28** 8058–63
- [19] Duduta M, Hajiesmaili E, Zhao H, Wood R J and Clarke D R 2019 Realizing the potential of dielectric elastomer artificial muscles *Proc. Natl Acad. Sci.* **116** 2476–2481
- [20] Duduta M, Clarke D R and Wood R J 2017 A high speed soft robot based on dielectric elastomer actuators 2017 *IEEE Int. Conf. on Robotics and Automation (ICRA)* pp 4346–51
- [21] Berlinger F, Duduta M, Gloria H, Clarke D, Nagpal R and Wood R 2018 A modular dielectric elastomer actuator to drive miniature autonomous underwater vehicles 2018 *IEEE Int. Conf. on Robotics and Automation (ICRA)* pp 3429–35
- [22] Zhao H, Hussain A M, Duduta M, Vogt D M, Wood R J and Clarke D R 2018 *Adv. Funct. Mater.* **28** 1804328
- [23] Evans M 1972 *J. Zool.* **167** 319–36
- [24] Evans M 1973 *J. Zool.* **169** 181–94
- [25] Ribak G and Weihs D 2011 *PLoS One* **6** e20871
- [26] Ribak G, Mordehay O and Weihs D 2013 *Bioinspir. Biomim.* **8** 036004
- [27] Kofod G 2008 *J. Phys. D: Appl. Phys.* **41** 215405
- [28] Rosset S, Araromi O A, Shintake J and Shea H R 2014 *Smart Mater. Struct.* **23** 085021
- [29] Fang W 1999 *J. Micromech. Microeng.* **9** 230
- [30] Timoshenko S 1925 *J. Opt. Soc. Am.* **11** 233–55
- [31] Niu X, Stoyanov H, Hu W, Brochu P and Pei Q 2013 *J. Polym. Sci. B* **51** 197–206
- [32] Roseau M 2012 *Vibrations in Mechanical Systems: Analytical Methods and Applications* (Berlin: Springer)
- [33] López-Puerto A, Avilés F, Gamboa F and Oliva A 2014 *Thin Solid Films* **565** 228–36
- [34] Meijer K, Rosenthal M S and Full R J 2001 Muscle-like actuators? A comparison between three electroactive polymers *Proc. SPIE* **4329** 7–16
- [35] Burrows M, Shaw S R and Sutton G P 2008 *BMC Biol.* **6** 41
- [36] Shian S, Diebold R M, McNamara A and Clarke D R 2012 *Appl. Phys. Lett.* **101** 061101
- [37] Hu W, Lum G Z, Mastrangeli M and Sitti M 2018 *Nature* **554** 81
- [38] Bolmin O, Duan C, Urrutia L, Abdulla A M, Hazel A M, Alleyne M, Dunn A C and Wissa A 2017 Pop! observing and modeling the legless self-righting jumping mechanism of click beetles *Conference on Biomimetic and Biohybrid Systems* (Berlin: Springer) pp 35–47